**Article:**
Khalid, N., Kim, J.Y., Ionescu, A. et al. (2018) Structure and magnetic properties of an epitaxial Fe(110)/MgO(111)/GaN(0001) heterostructure. Journal of Applied Physics, 123 (10). 103901. ISSN: 0021-8979

https://doi.org/10.1063/1.5022433

# Structure and magnetic properties of an epitaxial Fe(110)/MgO(111)/GaN(0001) heterostructure

N. Khalid, J.-Y. Kim, A. Ionescu, T. Hussain, F. Oehler, T. Zhu, R. A. Oliver, I. Farrer, R. Ahmad, and C. H. W. Barnes

Citation: Journal of Applied Physics **123**, 103901 (2018); doi: 10.1063/1.5022433
View online: https://doi.org/10.1063/1.5022433
View Table of Contents: http://aip.scitation.org/toc/jap/123/10
Published by the American Institute of Physics

# Structure and magnetic properties of an epitaxial Fe(110)/MgO(111)/GaN(0001) heterostructure

N. Khalid,[1,2] J.-Y. Kim,[1] A. Ionescu,[1,a)] T. Hussain,[3] F. Oehler,[4] T. Zhu,[4] R. A. Oliver,[4] I. Farrer,[1] R. Ahmad,[2] and C. H. W. Barnes[1]
[1]*Cavendish Laboratory, University of Cambridge, Cambridge CB3 0HE, United Kingdom*
[2]*Department of Physics, Government College University, 54000 Lahore, Pakistan*
[3]*Centre for Advanced Studies in Physics, Government College University, 54000 Lahore, Pakistan*
[4]*Department of Material Science and Metallurgy, University of Cambridge, Cambridge CB3 0FS, United Kingdom*

(Received 15 January 2018; accepted 6 February 2018; published online 9 March 2018)

We present the structural and magnetic properties of fully epitaxial Fe(110)/MgO(111)/GaN(0001) tunnel barrier structures grown by molecular beam epitaxy. *In-situ* reflection high-energy electron diffraction and *ex-situ* X-ray diffraction measurements indicate epitaxial Fe(110) films on top of an epitaxial 2 nm MgO(111) tunnel barrier on GaN(0001). X-ray reflectivity measurements confirm a roughness of approximately 0.3 nm and 0.7 nm for the MgO/GaN and the Fe/MgO interfaces, respectively. Results of *in-situ* magneto-optical Kerr effect measurements indicate that 1 nm thick Fe film shows signs of in-plane ferromagnetism at room temperature. Vibrating sample magnetometer measurements determine the saturation magnetisation of the 5 nm thick film to be $1660 \pm 100$ emu/cm$^3$ and show that this system has a predominant uniaxial anisotropy contribution despite the presence of cyclic twinned crystals. We estimate the values of effective uniaxial ($K_U^{\text{eff}}$) and cubic ($K_1^{\text{eff}}$) anisotropy constants to be $11700 \pm 170$ erg cm$^{-3}$ and $-3300 \pm 700$ erg cm$^{-3}$ by fitting the angular dependence of the magnetising energy. *Published by AIP Publishing.*
https://doi.org/10.1063/1.5022433

## I. INTRODUCTION

Epitaxial growth of ferromagnetic (FM) layers on semiconductor (SC) substrates is of paramount importance for creating sharp interfaces. These enable highly efficient spin transport through the structures without unwanted interface scattering and thus are a prerequisite for a high tunneling magneto-resistance (TMR) ratio.[1,2]

In the past three decades, epitaxial FM/SC heterostructures such as Fe/GaAs(001)[3,4] were extensively studied, in particular, for the realisation of the spin field-effect transistor (FET).[5] The injection, manipulation, and detection of a spin-polarized current in a SC material have the promising advantage of combining magnetic storage with electronic readout in a single device with multiple functionalities.[6] This paved the way for spintronics and new technologies such as the magnetic random access memory to emerge. An important obstacle in the realisation of the proposed spin FET was identified as the conductivity mismatch which exists between a FM metal and a SC which limits drastically the spin injection efficiencies.[7] This problem can be addressed by several possible means such as the insertion of an oxide tunneling barrier between the FM metal and the SC material.[8] Magnesium monoxide (MgO) has recently attracted much attention because epitaxial single crystalline MgO thin films act as a spin filter by favouring spin transport through similar symmetry states while suppressing others as predicted theoretically.[1,2] The spin filtering effect of MgO has been measured experimentally,[9,10] while the magnetic properties of the FM metal remained relatively unperturbed.[11,12] Gallium nitride (GaN), a wide-band gap semiconductor with $EG_s = 3.2$ eV at 300 K and less commonly known with a high thermal stability,[13] has found many applications in opto-electronics, high-frequency, and high-power microelectronics.[14] However, it is also an attractive substrate for spin transport[15] as spin lifetimes of 20 ns were previously measured[16] and a few hundred ns at room temperature (RT) were predicted for electrons injected into GaN,[17] which are three orders of magnitude larger than the spin lifetimes in GaAs.

In this paper, we present, to the best of authors' knowledge, the first experimental investigation of fully epitaxial Fe/MgO/GaN heterostructures grown by molecular beam epitaxy (MBE). The aim is to study the structural and magnetic properties of epitaxial ultra-thin Fe films on MgO tunnel barriers grown epitaxially on the GaN(0001) surface and hence to ascertain their potential for electrical spin transport device fabrication.

## II. EXPERIMENTAL PROCEDURE

The growth and *in-situ* measurements were carried out in a ultra-high vacuum (UHV) "multiple technique" molecular beam epitaxy (MBE) chamber, combining low-energy electron diffraction (LEED), reflection high-energy electron diffraction (RHEED), and longitudinal magneto-optical Kerr effect (MOKE) set-up, at a base pressure of $3 \times 10^{-10}$ mbar.

An epitaxial 2.1 $\mu$m thick GaN(0001) layer was grown directly on *c*-plane sapphire ($Al_2O_3$) substrates by metal organic chemical vapour deposition using a Thomas Swan $6 \times 2$ in. close-coupled showerhead reactor. By keeping a

a)Author to whom correspondence should be addressed: ai222@cam.ac.uk

high threading dislocation density of $2 \times 10^9$ per cm$^2$ (Fig. 1) for the GaN layer, the wafer bow after growth is minimal with a convex radius of curvature of about 62.5 m, as measured by *in-situ* optical monitoring (Laytec EpiCurve). High resolution X-ray diffraction (XRD) measurements with Cu $K_\alpha$ radiation of the (0004) GaN reflection (not shown) yielded $2\theta = 72.8952°$ and hence the lattice spacing $d = 1.2966$ Å and $c = 5.1864$ Å. The bulk value for the relaxed lattice parameter is $c = 5.1851$ Å (ICDD-PDF # 500792). Therefore, the estimated tensile strain in the out-of-plane direction is $dc/c = 2.5 \times 10^{-4}$ and the compressive strain in-plane is $da/a = -4.9 \times 10^{-4}$. We can hence conclude that the GaN layer is as close as possible to its bulk value and that the impact of strain on the structural and magnetic properties of the subsequently grown MgO and Fe layers has been minimised as far as possible. The grown substrates were then transferred in atmosphere to the MBE chamber.

Before being introduced into the UHV MBE chamber, the GaN(0001) surface was cleaned with acetone and isopropanol in an ultrasonic bath for 5 min in each solvent. After this, the substrate was rinsed in de-ionized water and dry-blown with $N_2$ gas. After transferring the GaN substrate to the MBE chamber through a load-lock, the substrate temperature was increased to 250 °C for 30 min in order to obtain a clean and ordered surface. For the epitaxial growth of the MgO tunnel barrier, we followed in parts the detailed growth study on MBE MgO growth as published by Losego *et al.*[18] After the surface preparation, a 2 nm thick MgO layer was grown by evaporating directly from a high-purity (99.999%) single MgO crystal, contained in a Ta crucible. The deposition rate for MgO growth was 0.3 monolayer per minute (ML/min) in $4.2 \times 10^{-8}$ mbar partial pressure of oxygen ($O_2$), while the substrate was kept at RT. After the MgO deposition, Fe layers with thicknesses ranging from nominally 1 to 5 nm were deposited at RT from a 99.999% pure Fe source in an e-beam evaporator at a growth rate of 0.6 ML/min. The base pressure of the chamber was around $2 \times 10^{-10}$ mbar, and the $O_2$ partial pressure was estimated to be at least below $1 \times 10^{-9}$ mbar during the Fe deposition

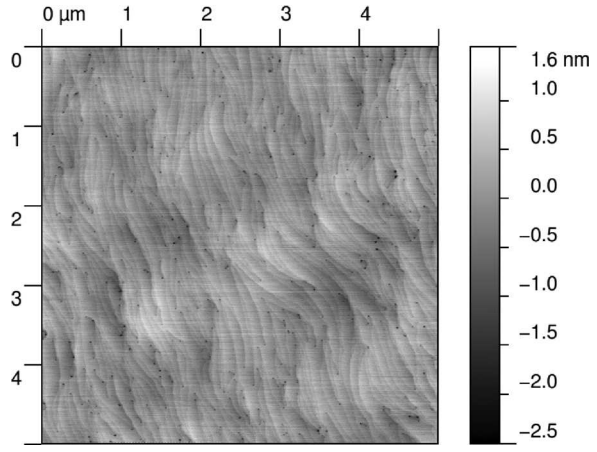


FIG. 1. 5 × 5 $\mu$m$^2$ atomic force micrograph of the surface of the GaN(0001) template. Black spots indicate dislocations. The bar on the right indicates the contrast scale.

according to our previous calibration. A quartz microbalance, calibrated against X-ray reflectivity (XRR) with an accuracy of $\sim \pm 10\%$ in the thickness estimation, was employed to monitor the deposition rate *in-situ*. To prevent the oxidation of the Fe film for *ex-situ* measurements, the sample was finally capped with a protective 7 nm Au layer. All *in-situ* MOKE measurements were performed at RT and prior to the Au capping layer deposition. *Ex-situ* characterization of the sample was conducted by X-ray diffraction (XRD) and X-ray reflectivity (XRR) for its structural and interface properties on a Bruker D8 Discover diffractometer. *Ex-situ* magnetic measurements at RT were performed by using a Microsense (model EVX) vibrating sample magnetometer (VSM).

## III. RESULTS AND DISCUSSION

Fe(110)/MgO(111) epitaxial films were epitaxially grown on a GaN(0001) substrate. Figure 2(a) presents a hexagonal LEED pattern of the GaN(0001) surface, acquired at the beam energy of 180 eV after the surface preparation. LEED was used to check the crystalline order of our substrates and film surfaces. We obtained sharp spots exhibiting hexagonal symmetry as expected for a GaN(0001) surface, with a low background intensity. Figures 2(b)–2(h) present the evolution of the RHEED patterns for the sample before, during and after MgO and Fe deposition. The incident electron beam at the energy of 15 keV was parallel to the "*a*" axis, GaN $[11\bar{2}0](0001)$.

The RHEED pattern with faint Kikuchi lines from the GaN(0001) surface, as shown in Fig. 2(b), indicates a high quality, smooth, and long range ordered single crystalline surface in agreement with the LEED image [Fig. 2(a)]. From the RHEED image shown in Fig. 2(c), taken after the deposition of 2 nm MgO, we observe the epitaxial growth of the tunnel barrier MgO. There are two possible orientations of the growth of rocksalt-structure MgO on wurtzite-structure GaN according to Craft *et al.*[19] One possibility is the MgO $\langle 110 \rangle$ directions which lie along the GaN $\langle 11\bar{2}0 \rangle$ directions and the other one is the MgO $\langle 110 \rangle$ directions which lie along the GaN $\langle 1\bar{1}00 \rangle$ directions. The two orientations are nearly degenerate from a lattice match perspective with 6.9% tensile against 7.4% compressive stress, respectively. Craft *et al.*, while mentioning that it is difficult to speculate about a chemical preference between these two possibilities, obtained only the 6.9% tensile strain epitaxial in-plane relation. The atomic row spacing of our MgO film obtained from the RHEED patterns, as seen in Table I, also indicates the former case, with the following epitaxial relationship: $(111)\text{MgO}||(0001)\text{GaN}$; $[10\bar{1}]\text{MgO}||[11\bar{2}0]\text{GaN}$. The schematic is shown in Fig. 3.

We infer that the Fe films grow epitaxially on the MgO film from Figs. 2(d)–2(h).[20,21] With increasing Fe film thickness, the intensity of the specular spots increases relative to the other features, implying that the surface becomes thicker. Figure 2(h) shows the presence of additional streaks (indicated by black lines) which point to in-plane cyclic twinned (in-plane triplets) Fe crystals. The epitaxial relationships can be assumed as $(110)\langle 001 \rangle \text{Fe}||(111)\langle 1\bar{1}0 \rangle \text{MgO}$. Hauch

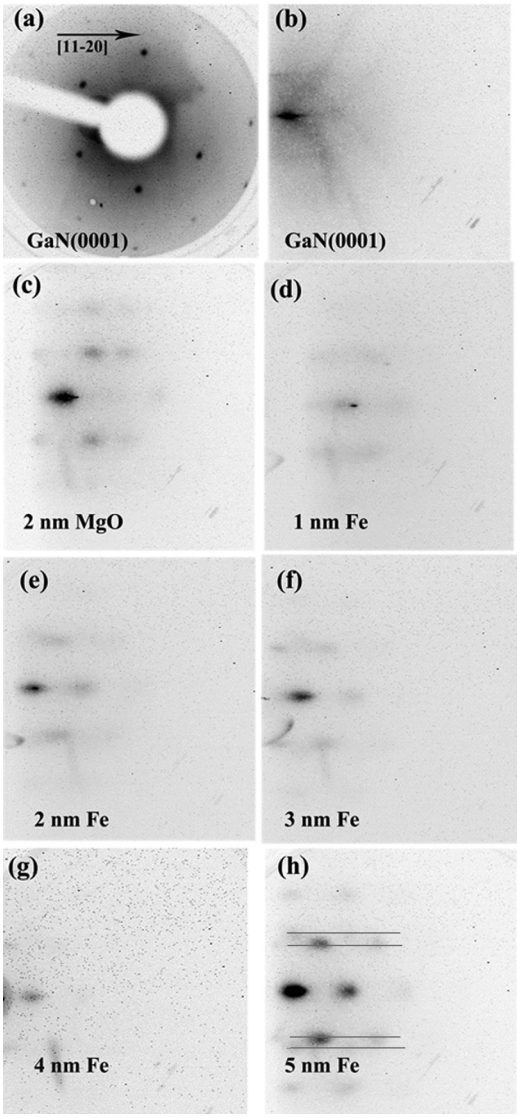


FIG. 2. (a) Hexagonal LEED pattern at 180 eV of the GaN(0001) surface before deposition. The arrow depicts the crystallographic in-plane direction. RHEED patterns taken at 15 keV beam energy along the $[11\bar{2}0]$ direction of the GaN substrate of (b) the GaN(0001) surface before deposition and (c) after deposition of 2 nm MgO, and (d)–(h) for 1, 2, 3, 4, and 5 nm thick Fe layers. The missing spots of the 4 nm film (g) are likely due to the misalignment of the electron beam.

*et al.*[22] and Lazarov *et al.*[23] studied the growth of Fe(110) films on MgO(111) and reported the same epitaxial relations.

The spacing between the streaks is inversely proportional to the atomic row spacing of the film. Hence, the corresponding lattice spacing can be estimated by measuring the streak separation. The observed values of the lattice

TABLE I. Relative RHEED streak separation and corresponding lattice spacing (measured and bulk) along GaN $[11\bar{2}0]$.

| | Relative RHEED spacing | Measured atomic row spacing (Å) | Bulk atomic row spacing (Å) |
|---|---|---|---|
| GaN | 1 | 2.76 (assumed) | 2.76 |
| MgO | $1.1 \pm 0.1$ | $2.5 \pm 0.3$ | 2.58 |
| Fe | $(1.2 \pm 0.1)$ and $(1.4 \pm 0.1)$ | $(2.3 \pm 0.2)$ and $(2.0 \pm 0.1)$ | 2.34 and 2.03 |

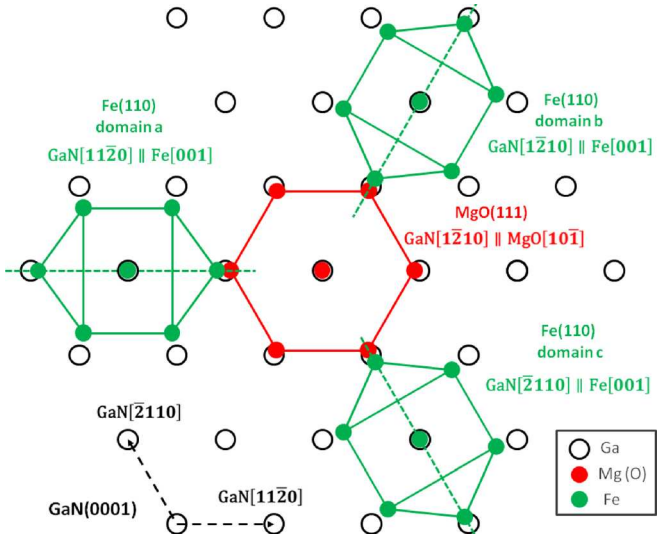


FIG. 3. Schematic diagram of three Fe lattices (green) on MgO (111) lattice planes (red) overlayed on a c-plane GaN lattice (black).

spacing/atomic row spacing determined from the RHEED images are shown in Table I. The lattice spacing along GaN $[11\bar{2}0]$ calculated from the RHEED patterns corresponds well to the theoretical values calculated from the schematics shown in Fig. 3. The proposed growth of our heterostructure, including the observed cyclic twinned (triplets) Fe crystal domains (green) on MgO(111) (red), is shown on the background GaN(0001) lattice. Despite the insertion of the MgO barrier, the crystallographic relations of Fe and GaN remain unaltered as compared to the epitaxial Fe/GaN(0001) structures.[24–26]

X-ray diffraction patterns were collected with a Bruker D8 Discover high-resolution X-ray diffractometer. Figure 4 shows the XRD scan of the completed heterostructure. Sharp diffraction peaks from the GaN(0002) and (0004) as well as $Al_2O_3$(0006) and Au(111) planes are visible in the XRD pattern. The MgO film is too thin (2 nm) for a visible XRD peak

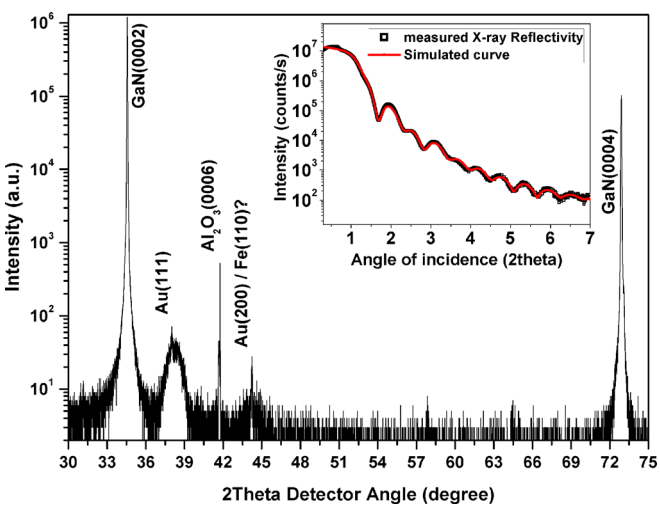


FIG. 4. X-ray diffraction pattern of the sample (7 nm Au/5 nm Fe/2 nm MgO/GaN(0001)). The inset shows X-ray reflectometry data of the same sample. The black open squares represent the measured XRR data and the red line represents the best fit.

TABLE II. The values of density, thickness, and roughness as estimated from XRR measurements.

| Material | Density (g/cm$^3$) | Thickness (nm) | Roughness (nm) |
|---|---|---|---|
| Au | 19.28 | 7.3 | 0.6 |
| Fe | 7.88 | 5.7 | 1.0 |
| MgO | 3.57 | 2.0 | 0.7 |
| GaN | 6.09 | … | 0.3 |

to appear. The small broad peak at ∼44.5° can be either Au(200) or Fe(110) or a superposition of both. If the Au would be polycrystalline the (200) peak should be half of (111) but this is not the case. So the scan is indicative of either a Au(111) textured or an Fe(110) film growth.

The X-ray reflectivity measurement was performed to estimate the thickness and interface roughness of the deposited films. The results obtained were fitted using the LEPTOS software. Obtained thickness and roughness values correspond well with the design values, as presented in Table II.

*In-situ* MOKE hysteresis loops of the Fe films were collected during the growth at RT with an applied field range of 500 Oe in the longitudinal geometry. To improve the signal-to-noise ratio, each loop presented was obtained by averaging over 100 times. Figures 5(a)–5(f) show the hysteresis loops and the measured coercivity of the 1 nm to 5 nm thick Fe films. As can be seen from Fig. 5, the hysteresis loop of the 1 nm Fe film demonstrates signs of ferromagnetism at RT with an in-plane magnetisation. As the thickness of the Fe layer, $t$, increases from 2 nm to 5 nm, the hysteresis loop area becomes wider and the coercivity increases. Interface defects, acting as pinning sites for the magnetisation reversal, could be the reason for the high coercivity of the 1 nm film compared to the thicker films. The coercivity value obtained for the 5 nm film was similar to the values reported previously.[26,27]

In order to study the competing magnetic anisotropies and to estimate the magneto-crystalline anisotropy constants, we performed VSM measurements at different in-plane angles $\varphi$ for the 5 nm sample. The saturation magnetisation ($M_s$) of the Fe film, measured at RT, was found to be 1659 ± 100 emu/cm$^3$, close to the bulk value of 1714 emu/cm$^3$. Figure 6 shows two VSM hysteresis curves taken along one of the $\boldsymbol{a}$ $[11\bar{2}0]$ and $\boldsymbol{m}$ $[1\bar{1}00]$ directions of the GaN(0001), demonstrating easy and hard axis switching, respectively.

In order to investigate the magnetic anisotropy in more detail, the VSM hysteresis loops were taken at every three degrees of the sample angle. Figures 7(a) and 7(b) show the polar plots of the squareness ratio ($M_r/M_s$) and coercivity ($H_c$) of the 5 nm thick Fe film, respectively. The squareness shows a clear uniaxial trend. The coercivity displays a similar uniaxial pattern, but with an underlying six-fold anisotropy, loosely aligning with the hexagonal symmetry of the base GaN substrate.

The magnetising energy, $\omega_m$, was determined by the method used in Bayreuther *et al.*[28] First, the *M-H* loops were made anhysteretic by shifting the up- and down-sweep scans by the corresponding coercivity. Field values of the anhysteretic loops were then integrated from zero magnetisation to

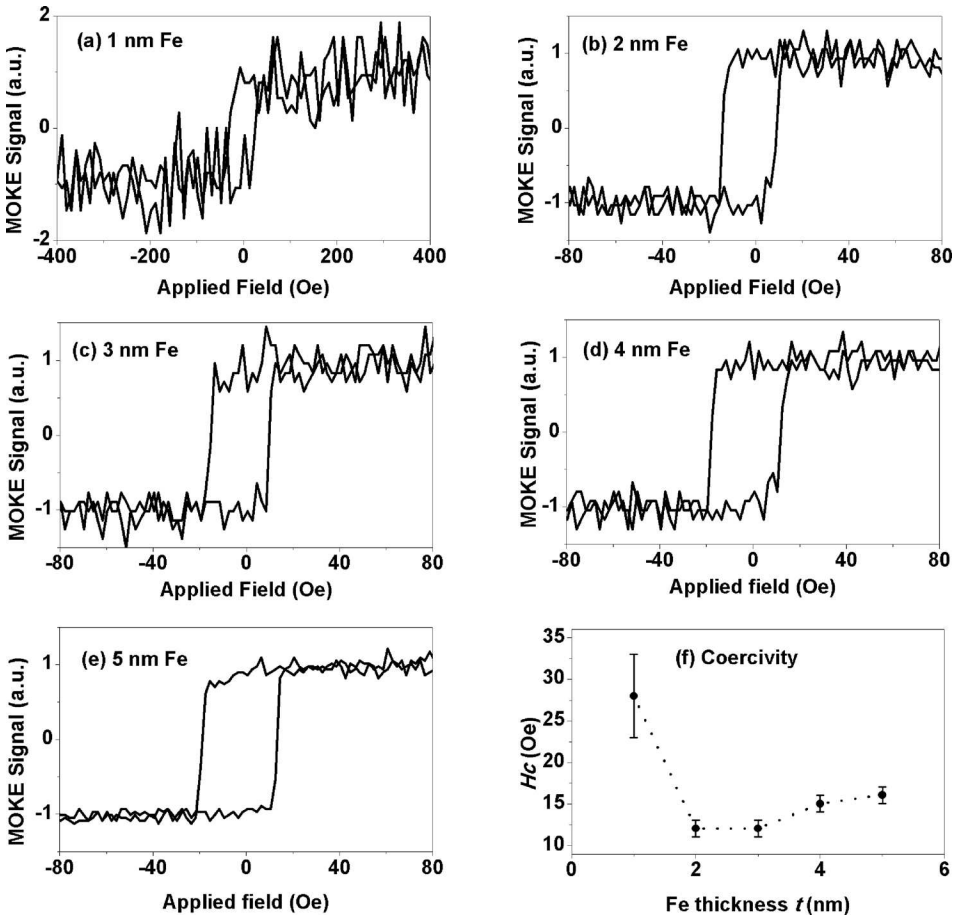


FIG. 5. *In-situ* MOKE *loops* (a)–(e) for 1, 2, 3, 4, and 5 nm thick Fe layers grown on MgO(111)/GaN(0001). (f) Variation in MOKE coercivity versus Fe films thickness. The dotted line represents a guide to the eye.

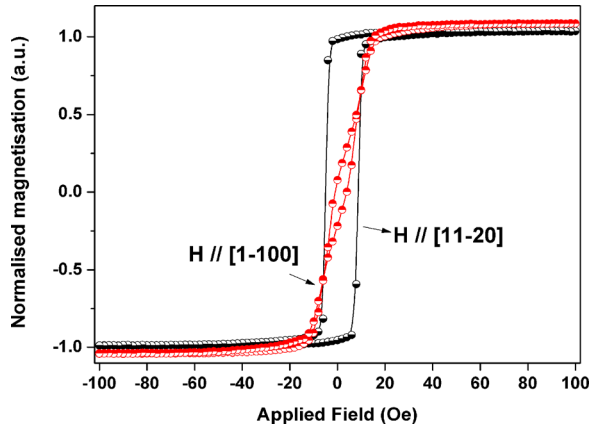


FIG. 6. The VSM hysteresis loops along one of the ***a*** $[11\bar{2}0]$ and ***m*** $[1\bar{1}00]$ axes of GaN(0001). Easy axis switching was observed along one of the *a*-axes, while the hard axis switching was measured along one of the *m*-axes.

positive saturated moments, as in $\int_0^{Ms} H.dM$, to obtain the values of $\omega_m$. The angular dependence of the magnetizing energy is displayed in Fig. 8 (black open squares). The overall magnetic anisotropy seems mainly uniaxial, with small variations which may represent the minor fourfold or sixfold contributions from the Fe(110) lattice.

In order to obtain anisotropy constants, Eq. (1) from Bayreuther *et al.*[28] was used to fit the magnetising energy

$$\omega_m^{Bay}(\varphi) = -\frac{K_1^{\text{eff}}}{4}\sin^2(2\varphi+\psi) + K_U^{\text{eff}}\sin^2(\varphi+\psi) + const., \tag{1}$$

where $K_1^{\text{eff}}$ and $K_U^{\text{eff}}$ are effective cubic and uniaxial anisotropy constants, $\varphi$ is the angle between magnetisation and the $[1\bar{1}00]$ GaN direction (corresponding to the zero sample angle), and $\psi$ is the angle between the magnetic easy axis and the sample zero angle. As can be seen in Fig. 8, a reasonable fit is obtained with the values of $K_1^{\text{eff}}$ and $K_U^{\text{eff}}$ being $-3300\pm700$ erg cm$^{-3}$ and $11700\pm170$ erg cm$^{-3}$, respectively. The about fourfold difference in the magnitude of the anisotropy constants confirms that the magnetic anisotropy is predominantly uniaxial.

Further attempts were made to improve the fitting so as to address the observed signs of four- and six-fold contributions in the magnetising energy. We employed the expression that Gao *et al.*[29] used successfully to describe the sixfold magnetic anisotropy of their 30 nm-thick Fe(110) film grown on GaN(0001). The expression involves three different terms to address the three twinned Fe(110) domains

$$\omega_m^{3D\_Gao}(\varphi) = A\times\omega_m^{Gao}(\varphi) + B\times\omega_m^{Gao}\left(\varphi+\frac{2\pi}{3}\right) + C \times\omega_m^{Gao}\left(\varphi+\frac{4\pi}{3}\right). \tag{2}$$

With

$$\begin{aligned}\omega_m^{Gao}(\varphi) = &-\frac{1}{32}K_1(7+4\cos2\varphi-3\cos4\varphi)\\ &+\frac{1}{128}K_2(2+2\cos2\varphi-2\cos4\varphi-\cos6\varphi)\\ &+\frac{1}{2048}K_3(123+88\cos2\varphi-68\cos4\varphi\\ &-24\cos6\varphi+9\cos8\varphi),\end{aligned} \tag{3}$$

where $A$, $B$, and $C$ are the weighted area factors for the three domain types, and $K_1$, $K_2$, and $K_3$ are the cubic anisotropy constants. We then replaced this expression with the effective cubic term in Eq. (1) to obtain the following fitting equation:

$$\omega_m^{Uni+3D\_Gao}(\varphi) = K_U^{eff}\sin^2(\varphi+\psi) + \omega_m^{3D\_Gao}(\varphi+\psi) + const. \tag{4}$$

As can be seen in Fig. 8, Eq. (4) seems to better address the higher order angular dependencies, where the values of $A$, $B$, and C are $0.30\pm0.06$, $0.00\pm0.40$, and $0.70\pm0.46$ and $K_1$, $K_2$, and $K_3$ are $6300\pm3800$ erg cm$^{-3}$, $(-2.6\pm2.7)\times10^5$ erg cm$^{-3}$, and $(1.4\pm1.8)\times10^5$ erg cm$^{-3}$. However, the numerical fit was found not to converge and the obtained area factors were significantly different from the equal area fractions of 0.33. It is also notable that the values of the cubic constants $K_1$, $K_2$, and $K_3$ deviate considerably from the values obtained in Gao *et al.*, as $4.7\times10^5$ erg cm$^{-3}$, $2.2\times10^4$ erg cm$^{-3}$, and $4.7\times10^5$ erg cm$^{-3}$, respectively. From this result, we conclude that the contribution of the higher order cubic components is negligible in our film, and the magnetic anisotropy is predominantly uniaxial. We speculate that the observed uniaxial anisotropy is an interfacial effect from the MgO/Fe interface, and a thickness-dependence study is necessary to quantify its effect. In addition, electron backscatter diffraction measurements would be insightful in determining the correct area fractions of each

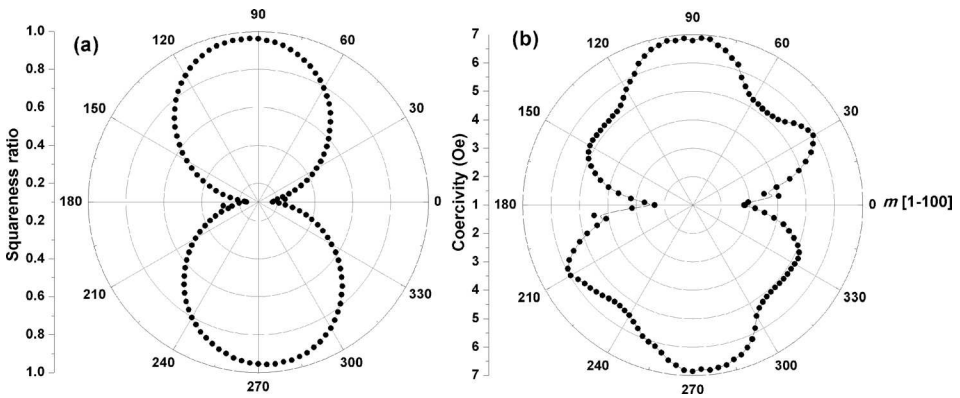


FIG. 7. Polar plots of the squareness ratio (a) and the coercivity (b) for the 5 nm thick Fe film. Zero degree corresponds to one of the GaN *m* axes.

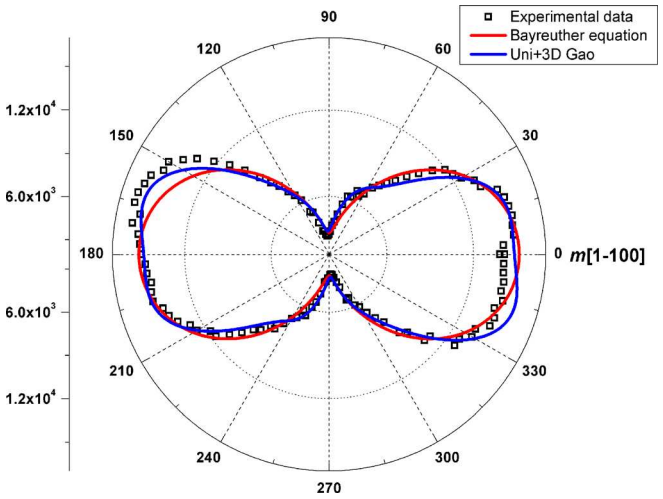


FIG. 8. Polar plot of the magnetising energy. The black open squares represent the experimental data. The red and the blue lines represent the numerical fit by the "Bayreuther" and "Uni + 3D Gao" expressions, respectively. Zero degree corresponds to one of the GaN ***m*** axes.

Fe(110) domains. For this thickness (5 nm) regime, the strongly uniaxial magnetic anisotropy could be useful in devices where pinning of the magnetisation is desirable.

## IV. CONCLUSIONS

We have studied the structural and magnetic properties of epitaxial Fe films grown on GaN(0001) with MgO(111) as a tunnel barrier. RHEED images indicated ordered and smooth Fe(110)/MgO(111) films as well as the presence of cyclic twinned crystals (triplets) of Fe on top of MgO(111) with the epitaxial relation as $(110)\langle 001\rangle$Fe $\|$ $(111)\langle 1\bar{1}0\rangle$ MgO $\|$ $(0001)\langle 1\bar{2}10\rangle$GaN. *In-situ* MOKE results indicated an in-plane ferromagnetism at RT for the thinnest Fe film studied (1 nm). VSM analysis yielded a magnetic moment of $1659 \pm 100$ emu cm$^{-3}$, close to the bulk value. The magnetic anisotropy was predominantly uniaxial as obtained from the magnetising energy calculation. Using phenomenological model, effective uniaxial ($K_U^{\text{eff}}$) and cubic ($K_1^{\text{eff}}$) anisotropy constants were estimated to be $11700 \pm 170$ erg cm$^{-3}$ and $-3300 \pm 700$ erg cm$^{-3}$.

## ACKNOWLEDGMENTS

One of the authors, Nida Khalid, would like to thank HEC (Higher Education Commission) Pakistan for their financial support.

[1]W. H. Butler, X.-G. Zhang, T. C. Schulthess, and J. M. MacLaren, Phys. Rev. B **63**, 054416 (2001).
[2]J. Mathon and A. Umerski, Phys. Rev. B **63**, 220403 (2001).
[3]G. Wastlbauer and J. A. C. Bland, Adv. Phys. **54**, 137 (2005).
[4]J.-B. Laloë, F. Van Belle, A. Ionescu, C. A. F. Vaz, M. Tselepi, G. Wastlbauer, R. M. Dalgliesh, S. Langridge, and J. A. C. Bland, IEEE Trans. Magn. **42**, 2933 (2006).
[5]S. Datta and B. Das, Appl. Phys. Lett. **56**, 665 (1990).
[6]F. G. Monzon, M. Johnson, and M. L. Roukes, Appl. Phys. Lett. **71**, 3087 (1997).
[7]G. Schmidt, D. Ferrand, L. W. Mollenkamp, A. T. Filip, and B. J. van Wees, Phys. Rev. B **62**, R4790 (2000).
[8]E. I. Rashba, Phys. Rev. B **62**, R16267(R) (2000).
[9]X. Jiang, R. Wang, R. M. Shelby, R. M. Macfarlane, S. R. Bank, J. S. Harris, and S. S. P. Parkin, Phys. Rev. Lett. **94**, 056601 (2005).
[10]A. Spiesser, S. Sharma, H. Saito, R. Jansen, S. Yuasa, and K. Ando, Proc. SPIE **8461**, 84610K (2012).
[11]J.-B. Laloë, A. Ionescu, S. Easton, N.-J. Steinke, T. J. Hayward, H. Kurebayashi, J. A. C. Bland, T. R. Charlton, R. M. Dalgliesh, and S. Langridge, Appl. Phys. Lett. **93**, 012505 (2008).
[12]J.-B. Laloë, A. Ionescu, T. J. Hayward, J. Llandro, J. A. C. Bland, and M. E. Vickers, Appl. Phys. Lett. **92**, 082505 (2008).
[13]C. Gao, O. Brandt, H.-P. Schönherr, U. Jahn, J. Herfort, and B. Jenichen, Appl. Phys. Lett. **95**, 111906 (2009).
[14]O. Ambacher, J. Phys. D: Appl. Phys. **31**, 2653 (1998).
[15]J.-Y. Kim, Ph. D. thesis, University of Cambridge, 2014.
[16]B. Beschoten, E. Johnston-Halperin, D. K. Young, M. Poggio, J. E. Grimaldi, S. Keller, S. P. DenBaars, U. K. Mishra, E. L. Hu, and D. D. Awschalom, Phys. Rev. B **63**, 121202 (2001).
[17]S. Krishnamurthy, M. van Schilfgaarde, and N. Newman, Appl. Phys. Lett. **83**, 1761 (2003).
[18]M. D. Losego, H. Spalding Craft, E. A. Paisley, S. Mita, R. Collazo, Z. Sitar, and J.-P. Maria, J. Mater. Res. **25**, 670 (2010).
[19]H. S. Craft, J. F. Ihlefeld, M. D. Losego, R. Collazo, Z. Sitar, and J.-P. Maria, Appl. Phys. Lett. **88**, 212906 (2006).
[20]D. J. Keavney, E. E. Fullerton, and S. D. Bader, J. Appl. Phys. **81**, 795 (1997).
[21]W. Wulfhekel, M. Klaua, D. Ullmann, F. Zavaliche, J. Kirschner, R. Urban, T. Monchesky, and B. Heinrich, Appl. Phys. Lett. B **78**, 509 (2001).
[22]J. O. Hauch, M. Fonin, M. Fraune, P. Turban, R. Guerrero, F. G. Aliev, J. Mayer, U. Rüdiger, and G. Güntherodt, Appl. Phys. Lett. **93**, 083512 (2008).
[23]V. K. Lazarov, S. H. Cheung, S. A. Chambers, M. Gajdardziska-Josifovska, and A. Kohn, Microsc. Microanal. **13**, 1044 (2007).
[24]C. Gao, H.-P. Schönherr, and O. Brandt, Appl. Phys. Lett. **97**, 031906 (2010).
[25]C. Gao, O. Brandt, S. C. Erwin, J. Lähnemann, U. Jahn, B. Jenichen, and H.-P. Schönherr, Phys. Rev. B **82**, 125415 (2010).
[26]J.-Y. Kim, A. Ionescu, R. Mansell, I. Farrer, F. Oehler, C. J. Kinane, J. F. K. Cooper, N.-J. Steinke, S. Langridge, R. Stankiewicz, C. J. Humphreys, R. P. Cowburn, and S. N. Holmes, J. Appl. Phys. **121**, 043904 (2017).
[27]P. K. J. Wong, W. Zhang, X. Cui, I. Will, Y. Xu, Z. Tao, X. Li, Z. Xie, and R. Zhang, Phys. Status Solidi A **208**, 2348 (2011).
[28]G. Bayreuther, J. Premper, M. Sperl, and D. Sander, Phys. Rev. B **86**, 054418 (2012).
[29]C. Gao, C. Dong, C. Jia, D. Xue, J. Herfort, and O. Brandt, Phys. Rev. B **92**, 094404 (2015).